Temperature dependence of the formal reduction potential of putidaredoxin

Vytas Reipa, Marcia J. Holden, Martin P. Mayhew, Vincent L. Vilker *

Biotechnology Division, Stop 8312, National Institute of Standards and Technology, Gaithersburg, MD 20899, USA

Abstract

Putidaredoxin (Pdx), a [2Fe–2S] redox protein of size M_r 11 600, transfers two electrons in two separate steps from the flavin containing putidaredoxin reductase to the heme protein, cytochrome CYP101 in the P450cam catalytic cycle. It has recently come to light, through NMR measurements, that there can be appreciable differences in the Pdx conformational dynamics between its reduced and oxidized states. The redox reaction entropy, $\Delta S_{rc}^{0'} = (S_{Pdx^r}^{0'} - S_{Pdx^o}^{0'})$, as determined from measurements of the variation in formal potential with temperature, $E^{0'}(T)$, provides a measure of the strength of this influence on Pdx function. We designed a spectroelectrochemical cell using optically transparent tin oxide electrodes, without fixed or diffusible mediators, to measure $E^{0'}(T)$ over the temperature range 0–40°C. The results indicate that the redox reaction entropy for Pdx is biphasic, decreasing from -213 ± 27 J mol^{-1} K^{-1} over 0–27°C, to -582 ± 150 J mol^{-1} K^{-1} over 27–40°C. These redox reaction entropy changes are significantly more negative than the changes reported for most cytochromes, although our measurement over the temperature interval 0–27°C is in the range reported for other iron–sulfur proteins. This suggests that Pdx (and other ferredoxins) is a less rigid system than monohemes, and that redox-linked changes in conformation, and/or conformational dynamics, impart to these proteins the ability to interact with a number of redox partners. © 2000 Elsevier Science B.V. All rights reserved.

Keywords: Cytochrome P450; Ferredoxin; Reduction potential; Redox reaction entropy; Spectroelectrochemistry

1. Introduction

Putidaredoxin (Pdx) is a [2Fe–2S] redox protein of size M_r 11 600 that serves as an electron shuttle in the P450cam-catalyzed hydroxylation of camphor by *Pseudomonas putida*. Pdx transfers two electrons in two separate steps from the flavin protein, putidaredoxin reductase, to the heme protein, cytochrome P450cam (CYP101; EC 1.14.15.1). Other low potential iron–sulfur proteins can replace individual elec-

tron transfer steps, but to date no other protein has been reported that can perform the complete function of Pdx in the hydroxylation catalytic cycle. Spinach ferredoxin and bovine adrenodoxin can donate the first electron to P450cam but not the second electron, whereas reduced rubredoxin and cytochrome b_5, which are incapable of giving the first electron, can provide the second electron yielding the reaction products [1]. The two Pdx electron transfer reactions are tightly controlled by the redox potentials of the interacting proteins, which in turn are affected by substrate binding, spin state equilibria, and their association with one another [2]. The formal reduction potential ($E^{0'}$) for Pdx shifts upon binding to

* Corresponding author. Fax: +1-301-975-5449;
E-mail: vincent.vilker@nist.gov

CYP101 (substrate-bound) from −240 mV to −196 mV, while the reduction potential of CYP101 shifts upon binding of substrate from −303 mV to −173 mV (vs. NHE, room temperature). These redox changes switch on the first electron transfer from Pdx to CYP101. The binding constant between reduced Pdx (Pdx^r) and oxidized CYP101 is about 100 times larger than between these two proteins when both are in the oxidized state [3].

This report is part of our ongoing effort to investigate the relationship between the structural features of Pdx and its interaction with redox partners [4–6]. Information gleaned from measurements of the formal reduction potential will give insight into the electron transport activity that is critical to the function of P450 catalysis, as well as contributing to general understanding of structure–function in the broad family of iron–sulfur redox proteins [7–11]. NMR studies by Pochapsky and co-workers have led to a proposal that the slower protein dynamics and more compacted structure exhibited by reduced Pdx (relative to the oxidized form) could contribute to the tighter binding of Pdx^r to CYP101 by minimizing conformational entropy loss upon binding [12,13]. More recent NMR studies, involving amide proton exchange measurements by Lyons et al. [14] and ^{15}N NMR relaxation measurements showing decreased backbone dynamics for Pdx^r by our group [6], suggest a significant decrease in the μs to ms mobility upon reduction. Such coupling between protein dynamics and changes in oxidation state could provide a mechanism for binding regulation without large conformational changes.

Measurements of $E^{0'}$ as a function of temperature are difficult due to slow approach to equilibrium, and restrictions on the range of solution conditions (temperature, ionic strength, pH) imposed by protein stability. Most known $E^{0'}$ measurements have been made by one of two broad methodologies: homogeneous or heterogeneous titration. In homogeneous titration, the redox reaction is driven using some chemical or biological reducing agent, and reaction progress is monitored potentiometrically or spectroscopically (UV-Vis, IR, Raman, EPR, etc.). Although in most cases high precision and reproducibility can be achieved, signal processing generally becomes too complex when temperature dependent studies are attempted by these methods. Heterogene-

ous titration methods have advanced significantly over the last 20 years, and have become the methods of choice in most cases since $E^{0'}$ is obtained directly from the voltammetric or spectroscopic response due to the redox reaction of the protein active center. However, proteins in general function poorly at many electrode surfaces due to large electron transfer distance, irreversible adsorption and/or protein denaturation. Surface properties of the electrode, such as charge density and its distribution, hydrophilicity and strength of interaction with the target protein, are important. In certain cases, a reversible protein response is achieved by employing charge transfer mediators or electrode surface modifiers (promoters). Data interpretation may be restricted by knowledge of the temperature dependent interactions of the promoter with the electrode surface and/or the redox protein.

Voltammetry is often used to evaluate $E^{0'}$ when a quasi-reversible response can be achieved. In this measurement, the so-called midpoint potential $E_{1/2}$ is determined from the peak separation of the cyclic voltammetry data [15]. The difference between $E_{1/2}$ and $E^{0'}$ is usually only a few millivolts, and depends on differences between the oxidized and reduced state molecular diffusion coefficients. Such measurements have been reported for proteins that undergo rapid electron exchange with various electrodes, including some iron–sulfur proteins [16–18], but only limited voltammetry data is available for putidaredoxin [19]. The primary difficulty is the absence of suitable electrode materials for sustained, reversible voltammetry responses. For Pdx, $E^{0'}$ has been determined using the dye photo-reduction method [2] which is not suitable for variable temperature studies.

Absorption spectroscopy can be utilized for redox titration whenever absorption spectra of oxidized vs. reduced protein show significant differences throughout the visible range. Spectroscopic measurements have been combined with optically transparent, thin layer electrode devices in order to measure $E^{0'}$ of various redox proteins [20–22]. Optically transparent metal oxide electrodes [23] can be especially suitable for these studies in some cases. Recently, we have reported the electrochemically driven CYP101 based bioreactor [24] using a thin film, antimony doped tin oxide electrode. These electrodes provided direct reduction of solution Pdx, thus sustaining the enzy-

matic cycle. Although the electrochemical response is rather slow, redox equilibrium is established within several minutes in a thin solution layer between electrodes. Also, the electrode material is almost totally transparent in the visible spectrum, therefore UV-Vis absorption measurements can be conveniently utilized for the protein oxidation state determination.

In the current investigation, we describe our efforts to measure the formal potential of Pdx as a function of temperature with the expectation of learning more about the behavior of this protein as a function of its oxidation state. An anaerobic non-isothermal spectroelectrochemical cell and measurement procedure enabled us to determine $E^{0'}(T)$ for Pdx. The thin layer cell with a non-protein adsorbing metal oxide electrode avoided the need for mediators or promoters, which always introduce the possibility of distorting the thermodynamic balance through introduction of undesirable interactions. The cell was used to reproduce similar measurements reported in the literature for the ferri/ferrocyanide and ferri/ferrocytochrome c redox couples. The redox reaction thermodynamic properties are calculated from these $E^{0'}(T)$ measurements.

2. Materials and methods[1]

2.1. Protein solutions

Pdx was prepared by heterologous expression of the protein on the plasmid pIBI25 in *Escherichia coli* (DH5α) cells. Cell growth and purification are described in detail by Grayson et al. [25]. In brief, the bacterial cells containing the plasmid were grown in batch culture on rich medium supplemented with ampicillin to maintain the plasmid. After overnight growth, the cells were harvested and the Pdx protein released from the cells by a combination of freeze–thaw and lysozyme–DNase treatment. The protein

was purified using two column chromatography steps (all column packings were obtained from Pharmacia Biotech, Uppsala, Sweden). First Pdx was loaded on a DEAE Fast Flow Sepharose (anion exchange) column and eluted with a KCl gradient. The protein was concentrated and placed on a Sephacryl S200 (gel filtration, size exclusion) column, and eluted. Spectroscopic methods were used to determine that the purity of Pdx was greater than 99 mol% with respect to other proteins. The protein was prepared for experiments by chromatography on Sephadex G25 Super Fine equilibrated with the buffer of choice. Alternatively, buffer exchange was effected by a concentration and dilution series using centrifugal membrane concentrators. Protein was stored at −80°C in 100 μl vials and thawed at room temperature prior to each experiment. For the cell validation tests, horse heart cytochrome c (Sigma Chemical, product number C3256) was used without further purification.

2.2. Electrochemical cell

The spectroelectrochemical cell was designed to allow for potentiostatic control of the protein solution within a thin layer gap, for variable electrolyte temperature settings from 0°C to 60°C, and for the ability to measure absorption over the near UV-Vis range during non-isothermal operation. Fig. 1 is a schematic of the cell body, which was manufactured from polystyrene with ports for three electrodes, pH microelectrode, gas purging, solution introduction, and uninhibited light passage.

The three electrode setup allows for control of the protein solution potential without the introduction of additional reducing or oxidizing agents. Electrochemical potential was maintained between the two 1×3 cm transparent antimony doped tin oxide (Delta Technologies, Stillwater, MN; product number CG-100SN) electrodes mounted face to face forming a 0.2 mm gap created by a Pt wire, which also served as a contact lead to the working electrode pair. The gap solution volume was about 100 μl, with the total solution volume in the cell equal to 0.5 ml. Another Pt wire, placed outside the gap, served as a counterelectrode. Solution pH was monitored continuously (Microelectrodes Inc., pH microelectrode MI-415, Londonderry, NH) and adjusted with small amounts

---

[1] Certain commercial equipment, instruments and materials are identified in this paper to specify adequately the experimental procedure. In no case does such identification imply recommendation or endorsement by the National Institute of Standards and Technology, nor does it imply that the material or equipment is necessarily the best available for the purpose.

of HCl or KOH. The electrodes were prepared for an experiment by several successive 5 min sonications in ethanol and water, followed by activation using a linear potential scan between -0.5 and $+1$ V at 0.1 V/s in 1 M HCl for 30 min. The working electrode assembly was mounted in a 1 cm plastic cuvette, equipped with two holes for the optical beam sealed from the solution by two O-rings. Prior to an experiment, the solution was slowly purged with argon gas for about 2 h. During measurements, the space above solution was kept filled with argon by carefully sealing the top with Parafilm (American National Can). Argon gas was sequentially passed through the oxygen scavenger (Oxyclear, Aldrich Chemical Co., Milwaukee, WI) followed by a distilled water column. In order to maintain non-isothermal conditions, the reference electrode (Ag/AgCl (3 M KCl) Abtech RE-803) was mounted at the end of the 40 cm long, 3 mm diameter Teflon tubing and kept at ambient temperature. A glass frit at the other end of the tubing formed a liquid junction with the thermostated protein solution. All potential values are reported on the NHE scale. Potential control was provided by an EG&G Model 273A electrochemistry system deployed in the chronoamperometric mode.

The cell was mounted in a two channel Ocean Optics PC2000 fiberoptic CCD spectrophotometer sample holder, modified for temperature dependent measurements. Each optical component in a sample holder was flushed continuously with dry argon to prevent fogging at the lower temperatures. Temperature in the cell was controlled using a water bath (Neslab RTE-100) and an external probe held in contact with the cell body via a heat sink compound (Dow Corning 340). The temperature difference between the solution and the probe was calibrated throughout the experimental range 0–40°C using a thermistor inside the cell. This difference was found to vary within ± 0.5°C.

2.3. Measurement procedure

Solutions were prepared in water, deionized by a Milli-Q water purification system. Analytical grade KCl and $MgCl_2$ were obtained from Mallinckrodt LLtd; reagent grade Tris–HCl and $K_3Fe(CN)_6$ were obtained from Sigma Chemical Co.

Performance of the non-isothermal cell was evaluated by testing against previously measured temperature dependences of the formal potentials of $[Fe(CN)_6]^{3-/4-}$ and of ferri/ferrocytochrome c [26, 27]. For both redox systems, at least three measurements were performed at each temperature, for both increasing and decreasing temperatures. The temperature dependent ferri/ferrocyanide midpoint potentials were determined from cyclic voltammograms of thoroughly deaerated, argon purged solutions (0.1 M KCl, 0.1 M $KHPO_4$, 1 mM $K_3Fe(CN)_6$, pH 7.5) recorded at 10 mV/s. Ferri/ferrocytochrome c formal potential in deaerated, argon purged solution (0.1 M $KHPO_4$, 100 μM cytochrome c, pH 7) was measured by optical absorption. After thorough deaeration, an initial reducing potential was applied in the interval from 0.0 to 0.1 V. Potential was held constant until the solution volume between the two electrodes was totally reduced as indicated by the stable reduced cytochrome c absorption spectrum [28], characterized by the maximum absorptivity at 550 nm and 520 nm. Next, potential was stepped to more positive values with simultaneous monitoring of the absorption spectra in order to ascertain the establishment of the equilibrium. In the region near equilibrium, the electrode potential was sequentially increased or decreased in 50 mV steps with a single step exposure between 1 min and 3 min, depending on the rate (variable) of reduction. A total of 27 potential steps were applied at each temperature which consisted of 12 steps in the negative direction, 12 in the positive and three steps at the extreme negative potential before reversal. Step exposure was varied to minimize hysteresis upon the reversal of potential. Potential variation limits were adjusted for each temperature accordingly in order to keep $E^{0'}$ approximately in the middle of the measurement interval. Absorption data were continuously collected for 30 s intervals at the end of each potential step. The oxidized/reduced protein concentration ratio was calculated from the absorbance differences at $\lambda = 520$ and 550 nm. Next, log C_{ox}/C_{red} was plotted against electrode potential to check for linearity and slope consistency with Nernst's equation.

The Pdx formal potential was measured in solution containing 0.15 M KCl, 0.01 M $MgCl_2$, and 200 μM Pdx buffered with 0.0375 M Tris–HCl to pH 7.5. After thorough purging, the initial reducing potential

was applied in the interval of -0.4 to -0.5 V. Potential was held constant until the solution volume between the two electrodes was totally reduced as indicated by the stable reduced Pdx absorption spectrum (Fig. 3). Next, the potential was stepped in the positive direction with simultaneous monitoring of the absorption spectra. Electrode potential was sequentially increased or decreased in 20 mV steps. Exposure at each single step was 5–40 min. The pattern of potential stepping at each temperature was the same as in the cytochrome *c* measurements. Absorption data were collected continuously for 100 s

intervals at the end of each potential step. Pdx concentrations were determined from the oxidized minus reduced molar absorptivities ($\Delta\varepsilon_1 = 6.8$ mM^{-1} cm^{-1} at 455 nm and $\Delta\varepsilon_2 = 6.4$ mM^{-1} cm^{-1} at 415 nm) using the average of two readings. Background variation was accounted for by subtracting absorbance at $\lambda = 750$ nm for each spectrum. Each spectrum was an average of 100 scans, 1 s exposure each, acquired after the establishment of the equilibrium. At least three measurements were performed at each temperature for both increasing and decreasing temperatures.
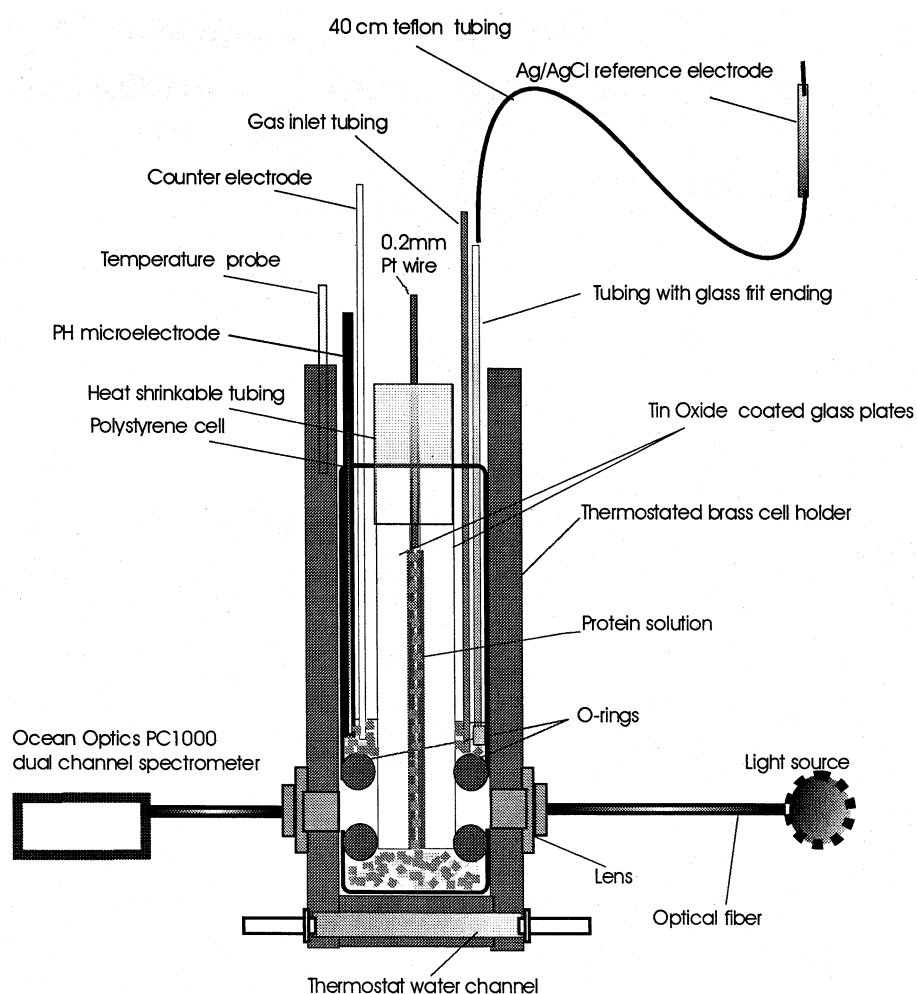

Fig. 1. Spectroelectrochemical cell (cross-section) used for temperature dependent redox titration. A polystyrene cell contains a pair of working electrodes made of 3 mm thick glass plates having antimony doped tin oxide coated inside surfaces. The electrodes are held together by Teflon shrink tubing with a 0.2 mm Pt wire between them. A thermostated brass cell holder is equipped with optical fiber connectors (Ocean Optics, Dunedin, FL) for monitoring optical absorption of solution in the gap between the transparent working electrodes. Spectrometer drift was compensated using a second channel connected to the light source through a bifurcated optical fiber. Reference electrode connection to the cell is accomplished through the 40 cm 3 M KCl solution filled Teflon tubing.

3. Results and discussion

We first tried to measure the redox potential of Pdx by heterogeneous titration using cyclic voltammetry (CV) with an organically modified gold electrode [19]. Drawbacks to this technique include the instability of the organic layer [29], which results in a non-persistent electrochemical response that obviates the usefulness of this method for measuring $E^{0'}(T)$. CV was also tried with an antimony doped tin oxide electrode with the intent to eliminate or minimize Pdx degradation that occurs on bare gold. However, we were unable to obtain a satisfactory electrochemical response throughout the whole temperature range, so that reliable formal potentials could not be determined from voltammetry curves. This led us to design a thin layer spectroelectrochemical cell using the transparent tin oxide electrodes, thereby permitting Pdx oxidation state changes to be obtained directly from optical absorbance spectrum. The thin layer geometry facilitates control of protein solution redox composition by gradual electrochemical reduction of the solution volume trapped in the narrow gap. The solution spectral analysis is performed after establishment of equilibrium, which is approached from both low and high initial poten-
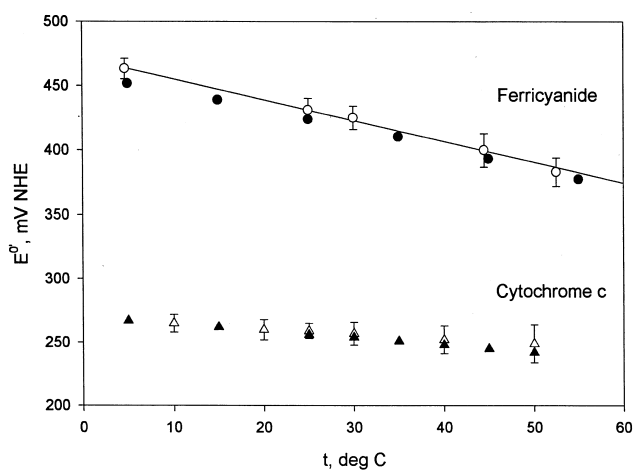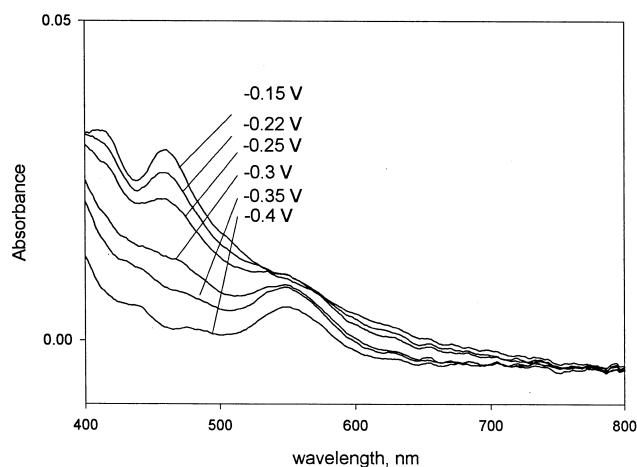

Fig. 3. Pdx visible absorption spectra at different electrode potentials and 25°C. Argon purged solution contained 200 μM Pdx in 0.15 M KCl, 0.01 M MgCl$_2$ and 0.0375 M Tris–HCl, pH 7.5.

tials. Absence of free or immobilized mediator dyes avoided spectral and chemical interference such as those experienced when working with optically transparent, thin gold film electrodes [22]. Our measured Pdx potential at 25°C was found to be −0.23 V (vs. NHE) which agrees well with the reported photochemical titration value ($E^{0'} = -0.24$ V) for Pdx at room temperature [2], although direct comparison is complicated due to different buffers and the uncertainty in the titration temperature.

The ability of the cell of Fig. 1 to maintain a stable temperature and redox environment during an electrochemical reaction was tested by measuring the temperature dependence of the formal potential of the ferro/ferricyanide couple over 0–60°C using cyclic voltammetry. As seen in Fig. 2, our $E^{0'}(T)$ measurements agreed with those of Koller and Hawkridge [26] to within 5 mV throughout the temperature range. The ferro/ferricyanide reaction entropy change, −149 J mol^{-1} K^{-1}, obtained using Eq. 1 and the slope of $E^{0'}(T)$ data in Fig. 2, agrees with previously reported values of Koller and Hawkridge (−37 eu, or −155 J mol^{-1} K^{-1}) [26], and with reports of Chi and Dong (−149 J mol^{-1} K^{-1}) [28]. We also measured $E^{0'}(T)$ of horse heart cytochrome c using absorbance at 520 nm and 550 nm for determination of the oxidation state. Again, our measurements are in good agreement with the previous report [26].
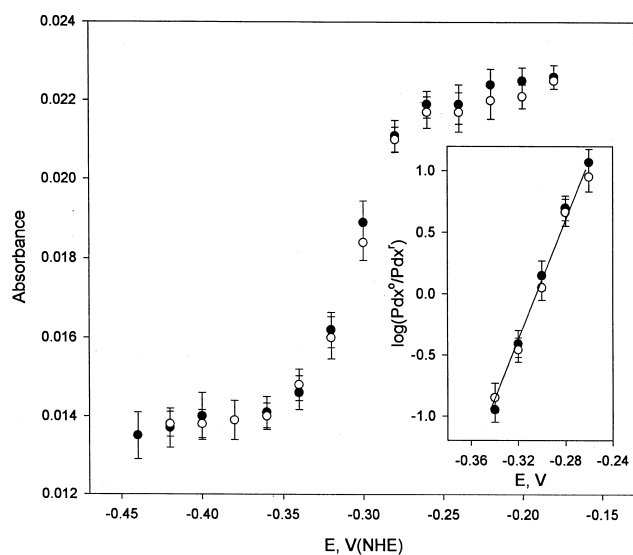
The visible absorption spectra of Pdx as recorded

Fig. 2. Temperature dependence of the formal potential of ferricyanide (○) and horse heart cytochrome c (△). Ferri/ferrocyanide measurements were made by cyclic voltammetry at a sweep rate of 10 mV/s in a solution of 0.1 M KCl, 0.1 M KHPO$_4$, 1 mM K$_3$Fe(CN)$_6$, pH 7.5; Ferri/ferrocytochrome c measurements were made from absorption spectra (520 nm and 550 nm) in a solution of 0.1 M KHPO$_4$, 100 μM cytochrome c, pH 7. Filled symbols are data from Koller and Hawkridge [26].

Fig. 4. Pdx titration curve obtained from absorbance at $\lambda = 455$ nm as measured in the spectroelectrochemical cell with tin oxide electrodes at 40°C. Solid circles are measurements made for potential changing in the negative direction, open circles signify positive direction. Solution conditions same as in Fig. 3. The half cell reaction is given by $Pdx^{ox} + e^- = Pdx^{red}$ and the potential by Nernst equation: $E = E^{0\prime} - 2.3\, RT/nF \log [Pdx^o]/[Pdx^r]$. Inset shows Nernstian plot for concentration ratios obtained from absorption differences between the oxidized and reduced species at 455 nm.

in our spectroelectrochemical cell are shown for several electrode potentials in Fig. 3. The absorbance maxima for oxidized Pdx observed at $E = -0.15$ V and wavelengths 415 nm and 455 nm are known to arise from Fe–S charge transfer excitations [30]. Upon gradual reduction to more negative potentials, these bands lose intensity and a band emerges at 540 nm which is characteristic of the reduced state. The visible spectra of Pdx did not change significantly with time for samples used in the $E^{0\prime}(T)$ determinations. However, after 3 h exposure at 40°C, visible spectra demonstrated gradual decay in absorptivity throughout the whole range, indicating denaturation and/or chromophore separation. We limited exposure in the runs at higher temperatures to less than 2 h.

We have calculated the oxidized/reduced protein concentration ratio from the absorbance differences at $\lambda = 415$ and 455 nm (Fig. 4). Next, log [Pdx^o]/[Pdx^r] was plotted against the electrode potential (inset in Fig. 4). The linear relationship indicates that the Nernst equation is a valid interpretation, so that

the log-zero intercept corresponds to equal concentrations of oxidized and reduced species, thus providing the value of the formal potential $E^{0\prime}$. The slope varied from 50 mV/dec at 2°C to 76 mV/dec at 40°C. There was no systematic variation of this slope with temperature, and the range of values corresponds to about 1 ± 0.15 electrons transferred in the Pdx redox reaction over the experimental temperature range.

The formal potential for Pdx was determined over the temperature range 0–40°C. At each temperature indicated in Fig. 5, measurements were made first from low to high temperature, and then from high to low temperature. The cycle was repeated a total of three times. Equilibrium for each measurement was approached from both the low and high potential direction. Average values of $E^{0\prime}$ and standard devia-
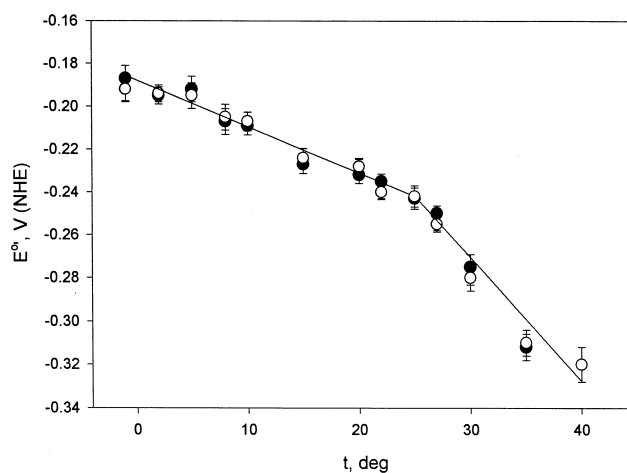

Fig. 5. Pdx formal potential as a function of temperature, $E^{0\prime}(T)$, from spectroelectrochemical titration. Open circles are measurements made when temperature of the cell is being increased from the previous measurement; solid circles are measurements made when temperature is changed in the decreasing direction. Each point is the average of three measurements. Error bars were calculated from standard deviation. Solid lines indicate the least squares linear fit of the experimental data. Temperature (°C), formal potential (V vs. NHE) for increasing temperature data: 0, −0.192 (±0.006); 2, −0.194 (±0.006); 5, −0.195 (±0.006); 8, −0.205 (±0.004); 10, −0.207 (±0.005); 15, −0.224 (±0.004); 20, −0.228 (±0.005); 22, −0.240 (±0.003); 25, −0.242 (±0.004); 27, −0.255 (±0.004); 30, −0.280 (±0.004); 35, −0.310 (±0.003); 40, −0.320 (±0.007). Values for decreasing temperature data: 35, −0.312 (±0.006), 30, −0.275 (±0.006); 27, −0.250(±0.004), 25, −0.243 (±0.005), 22, −0.235 (±0.004), 20, −0.232 (±0.004); 15, −0.227 (±0.004); 10, −0.209 (±0.004); 8, −0.207 (±0.006); 5, −0.192 (±0.006); 2, −0.195 (±0.004); 0, −0.187 (±0.006).

tions are plotted in Fig. 5. A most notable feature of these measurements is the biphasic behavior of $E^{0'}(T)$ centered around 27°C. Similar behavior has been reported for some *c*-type cytochromes [28,31–35] and has been ascribed to changes in protein conformation with change in oxidation state. Out of several measurements made on iron–sulfur proteins [16–18,36–39], there is the single report of biphasic behavior for the [4Fe–4S] ferredoxin from the hyperthermophile *Pyrococcus furiosus* [38]. This measurement was based on interpretation of potentiometric EPR spectroscopy data, and has not been reproduced by electrochemical methods [18,39].

The temperature dependence of the protein formal reduction potential provides a direct estimate of the electron transfer reaction entropy, $\Delta S_{rc}^{0'}$, when measured in a non-isothermal cell:

$$\Delta S_{rc}^{0'} = nF \left(\frac{\delta E^{0'}}{\delta T} \right)_P = (S_{Pdx^r}^{0'} - S_{Pdx^o}^{0'}) \qquad (1)$$

From the two distinct slopes for $E^{0'}(T)$ shown in Fig. 5, the biphasic behavior in the redox reaction entropy gives:

$$\Delta S_{rc}^{0'} = -213 \pm 27 \text{ J mol}^{-1} \text{ K}^{-1}, \quad 0 < t < 27°C$$

$$\Delta S_{rc}^{0'} = -582 \pm 150 \text{ J mol}^{-1} \text{ K}^{-1}, \quad 27 < t < 45°C$$

The complete electrochemical cell reaction [31] due to Pdx reduction is: $Pdx^o + 1/2H_2 \rightarrow Pdx^r + H^+$ so that at 25°C, the cell reaction standard entropy change is $\Delta S^{0'} = \Delta S_{rc}^{0'} - 65.2$ J mol^{-1} K^{-1}, and the standard enthalpy and free energy changes are given by; $\Delta H^{0'} = \Delta G^{0'} - T\Delta S^{0'}$ and $\Delta G^{0'} = -nFE^{0'}$. For our measurements, these quantities are: $\Delta G^{0'} = 21 \pm 5$ kJ mol^{-1}, $\Delta S^{0'} = -278 \pm 27$ J mol^{-1} K^{-1}, and $\Delta H^{0'} = -62 \pm 12$ kJ mol^{-1}.

The reaction entropy we found for Pdx in the temperature interval from 0°C to 27°C is in the range reported for most other ferredoxins [9,11,17,18,36–39], but is significantly more negative than the value reported for most cytochromes [21,28,31–35]. Comparing our Pdx measurements with those for [2Fe–2S] ferredoxins that are most similar in size and function (carriers of reducing equivalents to oxygenase redox partners), we find close agreement with the determinations for adrenodoxin ($M_r = 14\,000$; $E^{0'} = -254$ mV; $\Delta S_{rc}^{0'} = -209$ J mol^{-1} K^{-1}; $\Delta H^{0'} = -57$

kJ mol^{-1} [36]), and significant differences from those for benzene dioxygenase ferredoxin ($M_r = 11\,900$; $E^{0'} = -155$ mV; $\Delta S_{rc}^{0'} = -10$ J mol^{-1} K^{-1}; $\Delta H^{0'} = -7$ kJ mol^{-1} [17]).

Next, we consider the implications of the $E^{0'}(T)$ measurements for understanding Pdx function as an electron transfer protein. The protein induced effects on the iron–sulfur cluster reduction potential include: (i) alteration of cluster geometry and symmetry; (ii) electrostatic effects due to unit charges, fractional charges, and/or atomic cloud polarizability; (iii) structural changes between oxidized and reduced states (reorganization energy); (iv) solvent–cluster interactions; and (v) solvent shielding of protein–cluster electrostatic interactions [11]. Changes in the oxidation of the cluster may cause changes in any or all of these effects. These changes would be reflected in the redox reaction entropy and free energy measurements. In particular, redox linked conformational changes have been suggested previously for the [2Fe–2S] iron–sulfur proteins, adrenodoxin [36] and *Anabaena* ferredoxin [40]. It is also possible that differences in conformational dynamics between the oxidized and reduced state can lead to the measured entropy and free energy changes. This suggestion is supported by NMR studies on Pdx in our group [6], and in a report by Lyons et al. [14], where a significant decrease in mobility of the protein backbone is observed upon reduction. Such coupling between protein dynamics and changes in oxidation state could provide a mechanism for binding regulation without need for large changes in conformation.

Finally, we note that the reaction entropy measured here (−213 J mol^{-1} K^{-1}) is more than twice as negative as the partial entropy contribution calculated earlier [6] from ^{15}N NMR backbone dynamics measurements (−95 J mol^{-1} K^{-1}). This discrepancy is in contrast to the results for cytochrome b_5 by Dangi et al. [35] who found similar values for the reaction entropy determined by cyclic voltammetry $E^{0'}(T)$ data on the one hand, and by ^{15}N NMR backbone dynamics on the other. Taken together, these observations suggest that Pdx (and other ferredoxins) is a less rigid system than monoheme cytochromes, and that the other protein induced influences mentioned above are significant contributors too. This conclusion would be in keeping with the perception that these electron transfer proteins often must be

flexible enough to accommodate a number of redox partners. In the case of Pdx, both a flavin reductase and a P450 cytochrome must be accommodated at different points in the catalytic cycle. Tighter Pdx[r] binding to CYP101 may result from a more rigid structure thus minimizing the conformational entropy loss.

Acknowledgements

References

[1] J.D. Lipscomb, S.G. Sligar, M.J. Namtvedt, I.C. Gunsalus, J. Biol. Chem. 251 (1976) 1116–1124.

[2] S.G. Sligar, I.C. Gunsalus, Proc. Natl. Acad. Sci. USA 83 (1976) 1078–1082.

[3] M.J. Hintz, D.M. Mock, L.L. Peterson, K. Tuttle, J.A. Peterson, J. Biol. Chem. 257 (1982) 14324–14332.

[4] M.J. Holden, M.P. Mayhew, D. Bunk, A. Roitberg, V.L. Vilker, J. Biol. Chem. 272 (1997) 21720–21725.

[5] A.E. Roitberg, M.J. Holden, M.P. Mayhew, I.V. Kurnikov, D.N. Beratan, V.L. Vilker, J. Am. Chem. Soc. 120 (1998) 8927–8932.

[6] N. Sari, M.J. Holden, M.P. Mayhew, V.L. Vilker, B. Coxon, Biochemistry 38 (1999) 9862–9871.

[7] E.T. Smith, B.A. Feinberg, J. Biol. Chem. 265 (1990) 14371–14376.

[8] P.D. Swartz, T. Ichiye, Biochemistry 35 (1996) 13772–13779.

[9] A. Soriano, D. Li, S. Bian, A. Agarwal, J.A. Cowan, Biochemistry 35 (1996) 12479–12486.

[10] H. Shimada, S. Nagano, Y. Ariga, M. Unno, T. Egawa, T. Hishiki, F. Masuya, T. Obata, T. Horiuchi, J. Biol. Chem. 274 (1999) 9363–9369.

[11] F. Capozzi, S. Ciurli, C. Luchinat, Struct. Bond. 90 (1998) 127–160.

[12] T.C. Pochapsky, G. Ratnaswamy, A. Patera, Biochemistry 33 (1994) 6433–6441.

[13] T.C. Pochapsky, T.A. Lyons, S. Kazanis, T. Arakaki, G. Ratnaswamy, Biochimie 78 (1996) 723–733.

[14] T.A. Lyons, G. Ratnaswamy, T.C. Pochapsky, Protein Sci. 5 (1996) 627–639.

[15] D.H. Evans, S.A. Lerke, in: P.T. Kissinger, W.R. Heineman (Eds.), Laboratory Techniques in Electroanalytical Chemistry, Marcel Dekker, New York, 1996, p. 489.

[16] K. Nishiyama, H. Ishida, I. Taniguchi, J. Electroanal. Chem. 373 (1994) 255–258.

[17] T.A. Link, O.M. Hatzfeld, P. Unalkat, J.K. Shergill, R. Cammack, J.R. Mason, Biochemistry 35 (1996) 7546–7552.

[18] P.L. Hagedoorn, C.P.F. Driesses, M. Bosch, I. Landa, W.R. Hagen, FEBS Lett. 440 (1998) 311–314.

[19] L.S. Wong, V.L. Vilker, J. Electroanal. Chem. 389 (1995) 201–203.

[20] R. Szentrimay, P. Yeh, T. Kuwana, in: D.T. Sawyer (Ed.), Electrochemical Studies of Biological Systems, American Chemical Society, New York, 1977, pp. 143–169.

[21] V.T. Taniguchi, N. Sailasuta-Scott, F.C. Anson, H.B. Gray, Pure Appl. Chem. 52 (1980) 2275–2281.

[22] D.D. Schlereth, W. Mantele, Biochemistry 31 (1992) 7494–7502.

[23] F.M. Hawkridge, in: P.T Kissinger, W.R. Heineman (Eds.), Laboratory Techniques in Electroanalytical Chemistry, Marcel Dekker, New York, 1996, p. 283.

[24] V. Reipa, M.P. Mayhew, V.L. Vilker, Proc. Natl. Acad. Sci. USA 94 (1997) 13554–13558.

[25] D.A. Grayson, Y.B. Tewari, M.P. Mayhew, V.L. Vilker, R.N. Goldberg, Arch. Biochem. Biophys. 332 (1996) 239–247.

[26] K.B. Koller, F.M. Hawkridge, J. Am. Chem. Soc. 107 (1985) 7412–7417.

[27] F.M. Hawkridge, T. Kuwana, Anal. Chem. 45 (1973) 1021–1027.

[28] Q. Chi, S. Dong, J. Electroanal. Chem. 348 (1993) 377–388.

[29] L.S. Wong, V.L. Vilker, W.T. Yap, V. Reipa, Langmuir 11 (1995) 4818–4822.

[30] V.K. Yachandra, J. Hare, A. Gewirth, R.S. Czernuszewicz, T. Kimura, R.H. Holm, T.G. Spiro, J. Am. Chem. Soc. 105 (1983) 6462–6468.

[31] I. Taniguchi, M. Iseki, T. Eto, K. Toyosawa, H. Yamaguchi, K. Yasukouchi, Bioelectrochem. Bioenerg. 13 (1984) 373–383.

[32] I. Taniguchi, T. Funatsu, M. Iseki, H. Yamaguchi, K. Yasukouchi, J. Electroanal. Chem. 193 (1985) 295–302.

[33] P. Bertrand, O. Mbarki, M. Asso, L. Blanchard, F. Guerlesquin, M. Tegoni, Biochemistry 34 (1995) 11071–11079.

[34] B.A. Feinberg, X. Liu, M.D. Ryan, A. Schejter, C. Zhang, E. Margoliash, Biochemistry 37 (1998) 13091–13101.

[35] B. Dangi, J.I. Blankman, C.J. Miller, B.F. Volkman, R.D. Guiles, J. Phys. Chem. B 102 (1998) 8201–8208.

[36] Y.-Y. Huang, T. Kimura, Anal. Biochem. 133 (1983) 385–393.

[37] M. Asso, O. Mbarki, B. Guigliarelli, T. Yagi, P. Bertrand, Biochem. Biophys. Res. Commun. 211 (1995) 198–204.

[38] J.B. Park, C.L. Fan, B.M. Hoffman, M.W.W. Adams, J. Biol. Chem. 266 (1991) 19351–19356.

[39] P.S. Brereton, M.F.J.M. Verhagen, Z.H. Zhou, M.W.W. Adams, Biochemistry 37 (1998) 7351–7362.

[40] R. Morales, M.-H. Chron, G. Hudry-Clergeon, Y. Petillot, S. Norager, M. Medina, M. Frey, Biochemistry 38 (1999) 15764–15773.